



Crystal chemistry of natural occurring asbestos tremolite from calabrian ophiolites

Alessandro Pacella ^{1,*}, Paolo Ballirano ^{1,2}, Henrik Skogby ³,
Federica Angelosanto ⁴, Angelo Olori ⁴, Annapaola Cannizzaro ⁴,
Maria Rosaria Bruno ⁵, Francesco Sinopoli ⁵, Antonella Campopiano ⁴

¹ Department of Earth Sciences, Sapienza University of Rome, Piazzale Aldo Moro, 5-I-00185 Roma, Italy

² Laboratorio Rettoriale Fibre e Particolato Inorganico, Sapienza University of Rome, Piazzale Aldo Moro, 5-I-00185 Roma, Italy

³ Swedish Museum of Natural History, Department of Geosciences, Box 50007, SE-104 05 Stockholm, Sweden

⁴ Department of Medicine, Epidemiology, Occupational and Environmental Hygiene, National Institute for Insurance against Accidents at Work (INAIL), Rome, Italy

⁵ Department of Medicine, Epidemiology, Occupational and Environmental Hygiene, National Institute for Insurance against Accidents at Work (INAIL), Lamezia Terme, Italy

ARTICLE INFO

Submitted: March 2021

Accepted: April 2021

Available on line: July 2021

* Corresponding author:
alessandro.pacella@uniroma1.it

Doi: 10.13133/2239-1002/17410

How to cite this article:

Pacella A. et al. (2021)

Period. Mineral. 90, 307-316

ABSTRACT

The present work reports a detailed chemical and structural characterization of a fibrous tremolite sample from an abandoned serpentine quarry located in Mount Reventino (Calabria, Italy), by using SEM-EDS analysis, Mössbauer spectroscopy, and X-ray powder diffraction. Cell parameters, fractional coordinates and site scattering were refined using the Rietveld method. Results showed that the sample contains small amount of Fe, being the % ferro-actinolite content of ca. 3%. In particular, Fe²⁺ is preferentially allocated at M(1)+M(3) octahedral sites, and Fe³⁺ only occurs at M(2). Combining chemical, spectroscopic and structural data the following empirical formula has been derived: $A(Na_{0.124})_{\Sigma 0.124}M^{(4)}(Ca_{1.922}Na_{0.003}Fe^{2+}_{0.026}Mg_{0.049})_{\Sigma 2.000} [M^{(1)}(Mg_{1.960}Fe^{2+}_{0.040})_{\Sigma 2.000}M^{(2)}(Mg_{1.963}Fe^{3+}_{0.024}Fe^{2+}_{0.013})_{\Sigma 2.000}M^{(3)}(Mg_{0.931}Fe^{2+}_{0.069})_{\Sigma 1.000}] [T^{(1)}(Si_{3.946}Al_{0.024})_{\Sigma 3.970}T^{(2)}(Si_{4.000})] O_{22}O^{(3)}(OH_{2.000})_{\Sigma 2.000}$. Considering that both the presence of Fe and its coordination environment within the mineral structure are primary factors for pathological effects, the identification of Fe bearing asbestos tremolite in the investigated area may represent a potential hazard for human health.

Keywords: Tremolite; Naturally Occurring Asbestos (NOA); SEM-EDS; Mössbauer spectroscopy; Rietveld method.

INTRODUCTION

Naturally occurring asbestos (NOA) is a general term applied to the geologic occurrence of any of the six types of asbestos minerals (chrysotile, tremolite, actinolite, anthophyllite, riebeckite, and grunerite, with the last two commercially known as crocidolite and amosite,

respectively) occurring in rocks and soils as result of natural geological processes (Nichols et al., 2002; Lee et al., 2008; Harper, 2008). It is in fact well known that asbestos can be found as accessory minerals of mafic and ultramafic rock sequences (Pacella et al., 2010; Vignaroli et al., 2011, 2014). In ophiolite complexes,

the most abundant of these rocks, chrysotile, tremolite and actinolite asbestos frequently occur (Ross and Nolan, 2003). Ophiolites represent remnants of paleo-oceanic lithosphere consisting of pillow basalts, gabbros, serpentinites and basal peridotites that experienced a wide range of geological processes, such as shear deformation and fluid-rock interaction (Vignaroli et al., 2011, 2014).

In the Italian peninsula, especially in the Alps and the Apennines, there are several ophiolite outcrops rich both in serpentine and amphibole asbestos. In particular, the Piedmont region (NW Italy) has the largest occurrence, and an environmental problem was recently raised in Susa Valley by railway tunnel excavations through metamorphic formations, such as serpentinites, containing fibrous tremolite (Ballirano et al., 2008). Some other examples of NOA bearing rocks in other regions of Italy include, from north to south, the Natural reserve of Mount Rufeno in Latium (Burrigato et al., 2001), the Mount Reventino area (Sila Massif) and the Coastal Chain in Calabria (Bloise et al., 2014, 2016), and the Pollino Massif in Basilicata (Burrigato et al., 2010).

Ophiolitic rocks are of economic importance since they are commonly used as building and ornamental materials because of their physical and mechanical qualities such as strength, durability, and variety in appearance and colour (Marinos et al., 2006; Pereira et al., 2007). It must be pointed out that in serpentinite quarries, even if not operating for asbestos production, asbestiform minerals have been identified in the rocks (Gualtieri et al., 2020). Natural weathering and human activities, such as road construction, mining and agriculture, may disturb NOA bearing rocks or soils and result in airborne respirable fibres dispersed in the surrounding environment, therefore inducing potential human exposure (Langer, 2008; Cavallo and Rimoldi, 2013; Bloise et al., 2016).

NOA has started to capture the interest of the public opinion worldwide since epidemiological investigations highlighted an increased occurrence of malignant mesothelioma in the populations living within or near to NOA sites (Ross and Nolan, 2003; Pan et al., 2005). Consequently, in some states of the USA, such as Virginia, Maryland, Pennsylvania and California (El Dorado County), an asbestos exposure control plan has been instituted for construction activities (Ross and Nolan, 2003; Lee et al., 2008). It must be pointed out that in Italy the presence of fibrous tremolite in the soils of the towns of Lauria and Castelluccio Superiore (Basilicata) has been related to some pleural mesothelioma cases occurred in these rural communities (Pasetto et al., 2004). In addition, *in vivo* experiments highlighted that tremolite fibres from Lanzo Valley (Piedmont) are highly carcinogenic (Davis et al., 1991; Addison and McConnel, 2005). On this basis, dedicated work is required for NOA identification

and characterization in order to map possible sources and prevent, or at least reduce, the risk of exposure for both workers and general public (Decree of the Italian Environment Ministry, 18 March 2003, n° 101).

In the present work, tremolite fibres coming from an abandoned serpentine quarry in Mount Reventino (Calabria, Italy) are investigated by means of a well-tested multi-analytical approach. A complete crystal-chemical and structural characterization, including cation site partition and $\text{Fe}^{2+}/\text{Fe}^{3+}$ speciation has been obtained by combining SEM-EDS, Mössbauer and X-ray powder diffraction data. In fact, the detailed knowledge of those parameters is of paramount relevance for modelling the reactivity of such fibres the aim being the possible identification of potential risks posed to human health.

EXPERIMENTAL

Materials

The PL5 sample investigated in this work comes from an abandoned serpentine quarry located in the Mount Reventino area (Calabria, Italy, longitude $16^{\circ}18'44''$, latitude $39^{\circ}02'07''$), in the Northern sector of the Calabrian Peloritan Orogen (Figure 1). The Calabrian Peloritan Orogen represents a fragment of the European margin, which was thrust onto the Maghrebic-Sicilian and Apennine thrust-and-fold belt during the Europe-Apulia collision in Oligocene-Early Miocene (Amodio Morelli et al., 1976 and references therein; Vitale et al., 2013). According to Ogniben (1969), it consists of three main tectonic superimposed complexes that represent different paleogeographic domains, from top to bottom: the Calabride Complex made up of Hercynian and pre-Hercynian gneiss, granite and metapelite; the Liguride nappe (Tithonian-Neocomian) made up of a series of Alpine metamorphic units including a Cretaceous-Paleogene metapelitic-ophiolitic-carbonate assemblage; the Apennine Units Complex made up of Mesozoic sedimentary and metasedimentary successions (Trias-Miocene). Each tectonic complex was also further divided into different tectonic units (Amodio Morelli et al., 1976; Piluso et al., 2000; Cirrincione et al., 2015). The ophiolitic sequences of Mount Reventino belong to the Liguride complex and include mainly serpentinitized ultramafic rocks and ophicalcites, metabasalts and subordinately metadolerites, and a metasedimentary cover consisting of an alternation of metapelites, metarenites, and metalimestones (Piluso et al., 2000; Alvarez, 2005; Bloise et al., 2016).

Scanning Electron Microscopy (SEM) with energy dispersive spectroscopy (EDS)

Sample morphology was investigated from a fragment of the hand specimen, mounted on a stub and carbon coated, using a FE-SEM Merlin Zeiss. Selected electron

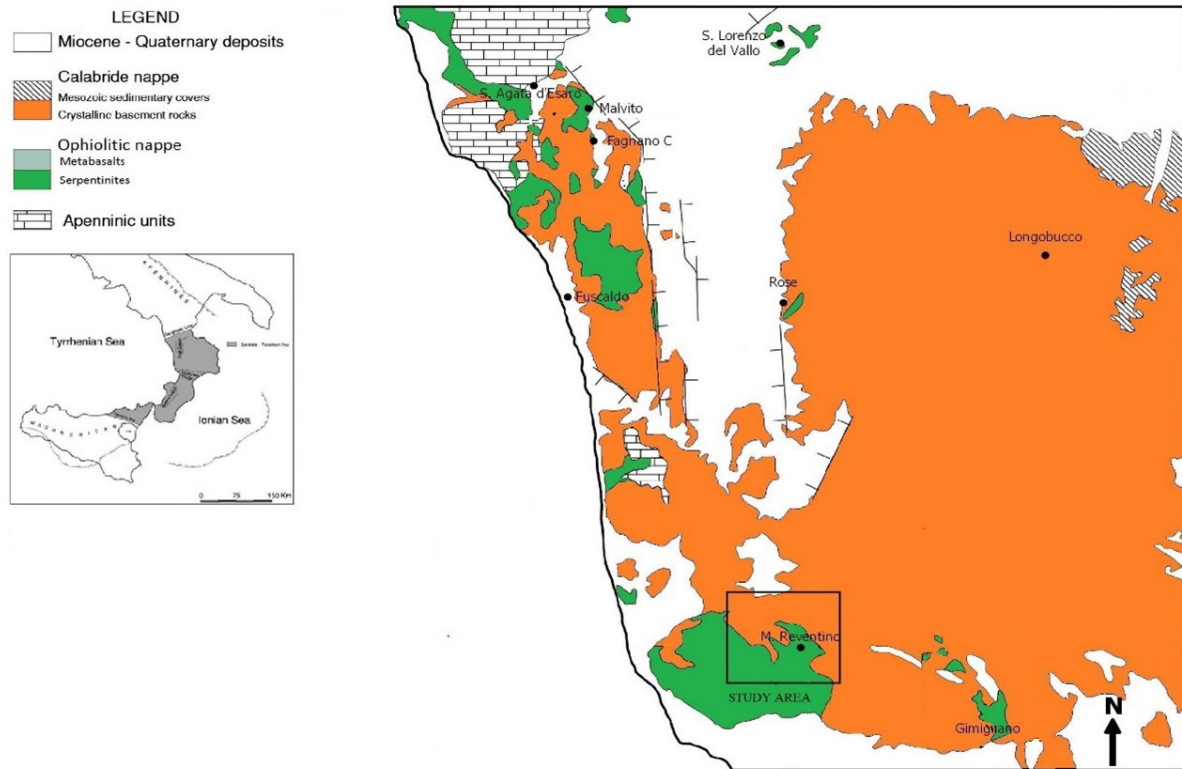


Figure 1. Geological sketch map of the northern Calabrian showing ophiolites occurrence and the location of the investigated asbestos sample. Modified from Punturo et al. (2015).

micrographs taken at different magnifications are reported in Figure 2. The average chemical composition of the fibres was determined from 9 analytical points using a Zeiss DSM 940A equipped with a standardized LINK EDS system. Analytical conditions were: 15 kV accelerating voltage and 3.4 μ A beam current. The following standards were used: wollastonite (Si $K\alpha$, Ca $K\alpha$), corundum (Al $K\alpha$), magnetite (Fe $K\alpha$), periclase (Mg $K\alpha$), orthoclase (K $K\alpha$), and jadeite (Na $K\alpha$). Table 1 shows the average chemical composition and crystal-chemical formula, normalized on the basis of 24 (O+F+Cl). Cations are reported in atoms per formula unit (apfu) and were assigned to the various sites following Hawthorne et al. (2012).

⁵⁷Fe Mössbauer Spectroscopy

A Mössbauer spectrum of the PL5 tremolite sample was acquired using a conventional spectrometer system operated in constant-acceleration mode. The Mössbauer absorber was prepared by grinding ca. 95 mg sample material together with 100 mg acrylic resin. This mixture was pressed to a 12 mm diameter disc under mild heating. The spectrum was measured at room temperature using a standard ⁵⁷Co source in a Rh matrix with a nominal activity of 50 mCi. Spectral acquisition was obtained over

1024 channels in the velocity range -4.2 to +4.2 mm/s, and the data was then calibrated against a spectrum of an α -Fe foil before folding and fitting using the software MossA (Prescher et al., 2012). The spectrum was fitted with one quadrupole doublet assigned to Fe³⁺ and three doublets assigned to Fe²⁺. Lorentzian line shapes, equal recoil-free fractions, and equal intensities of the quadrupole components were assumed in the fitting procedure. Figure 3 shows the ⁵⁷Fe Mössbauer spectrum of the sample. Table 2 reports the relevant hyperfine parameters of the spectral fitting.

X-ray Powder Diffraction

X-ray Powder Diffraction (XRPD) data were collected on a Bruker AXS D8 Advance operating in transmission mode, θ/θ geometry. The sample was ground and homogenised in an agate mortar and the powders were loaded in a 0.7 mm diameter boro-silicate glass capillary sealed at both ends. The instrument is fitted with incident-beam focussing Göbel mirrors and a VÅntec-1 position sensitive detector set to an opening angle of 6°. Soller slits are placed along both incident (2.3°) and diffracted (radial) beams. Data were measured in the 6-145° 2 θ angular range, 0.0218° 2 θ step size and 8 s counting time.

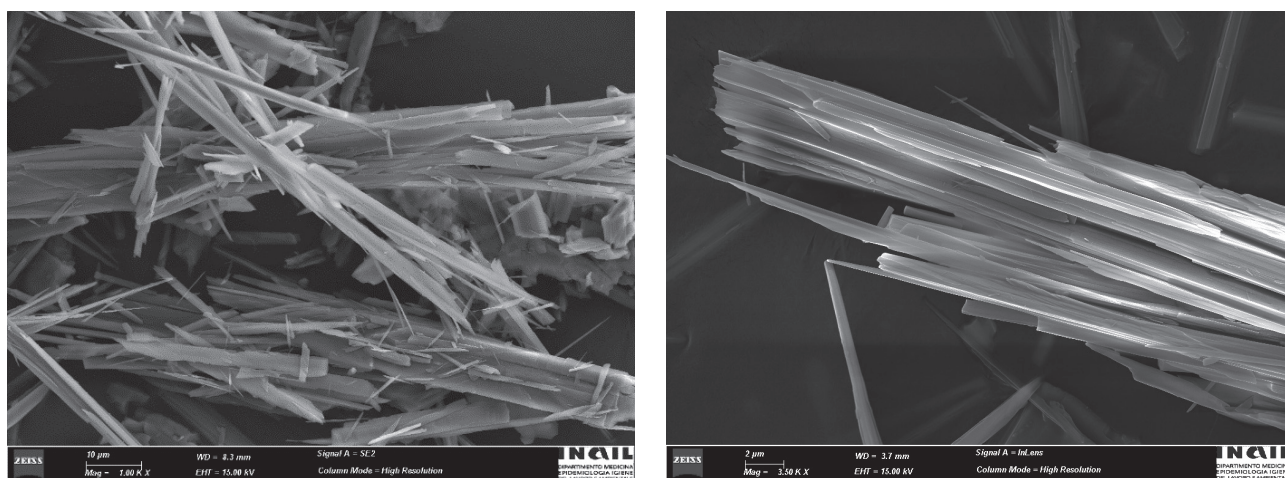


Figure 2. FE-SEM images of tremolite fibres at increasing magnification showing straight and rigid fibres aggregate in bundles.

Table 1. Chemical composition of the tremolite fibres sample from SEM-EDS data. Standard deviations are reported in brackets. $\text{Fe}^{3+}/\text{Fe}^{2+}$ from Mössbauer data.

Oxides	Wt%	Cations on basis of 24 (O,OH,F)**		
SiO_2	58.33(27)	T	Si	7.946(26)
Al_2O_3	0.15(10)		Al	0.024(17)
Fe_2O_3	0.23(3)		total	7.970(16)
FeO	1.30(19)	C	Fe^{3+}	0.024(3)
MgO	24.14(44)		Fe^{2+}	0.122(18)
CaO	13.17(55)		Mg	4.854(30)
Na_2O	0.48(18)		total	5.000(12)
H_2O^*	2.20	B	Fe^{2+}	0.026(4)
Total	100.00		Mg	0.049(64)
			Ca	1.922(82)
			Na	0.003(6)
			total	2.000(19)
		A	Na	0.124(48)
			total	0.124(48)

Note: *estimated from stoichiometry; **with OH = 2 apfu

Preliminary analysis of the pattern revealed the occurrence of minor calcite and serpentine-like phase(s). It should be mentioned that the occurrence of polygonal serpentine, chrysotile and fibrous antigorite has been reported from the Mount Reventino area (Bloise et al., 2014). Rietveld refinement was carried out using Topas V6 (Bruker AXS, 2016). The anisotropic line broadening, caused by the fibrous morphology, was modelled using the multi-

dimensional distribution of lattice metrics proposed by Stephens (1999). The equation of Sabine et al. (1998) for a cylindrical sample was used for modelling absorption effects. Preferred orientation was corrected using the normalized symmetrized spherical harmonics functions, described by Järvinen (1993), and selecting the number of terms (4th-order, eight refinable parameters) following the procedure described by Ballirano (2003). Parameters

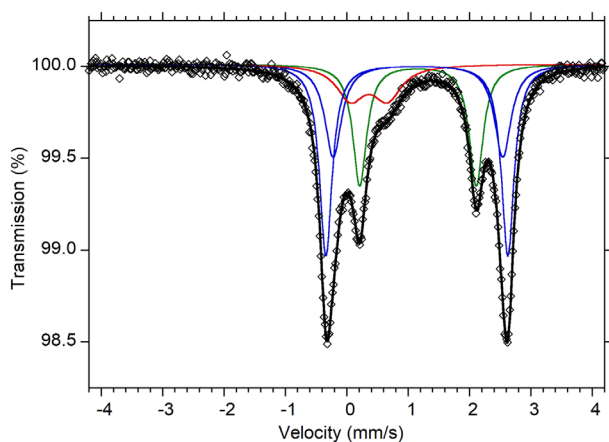


Figure 3. ^{57}Fe Mössbauer spectrum of tremolite obtained at room temperature. Fitted absorption doublets assigned to $\text{Fe}^{2+} M(1)+M(3)$ are indicated in blue color, $\text{Fe}^{2+} M(2)+M(4)$ in green color, and $\text{Fe}^{3+} (M2)$ in red color. Diamonds denotes measured spectrum, and black curve represents summed fitted spectrum.

refined to very small values as expected for a sample prepared as capillary. Starting structural data of tremolite were those of Pacella et al. (2020). Isotropic displacement parameters were kept fixed to the corresponding values. Refined structural parameters included fractional coordinates for all non-hydrogen atoms and site occupancy fraction (sof) of A, B and C sites. Structural data of calcite and serpentine-like phase(s) (approximated by a single antigorite $m=17$ polysome) were taken from Maslen et al. (1993) and Capitani and Mellini (2004), respectively. Only scale factors, cell parameters and peak shapes of these two phases were optimized as a part of the Rietveld refinement. Figure 4 shows the conventional Rietveld plots of the refinement of PL5. Table 3 lists cell parameters and volume of tremolite plus the agreement factors of the refinement, Table 4 reports the quantitative phase analysis (QPA) of the sample. Table 5 shows relevant bond distances of the structure of tremolite. CIF file is deposited as supporting material at the site of the journal.

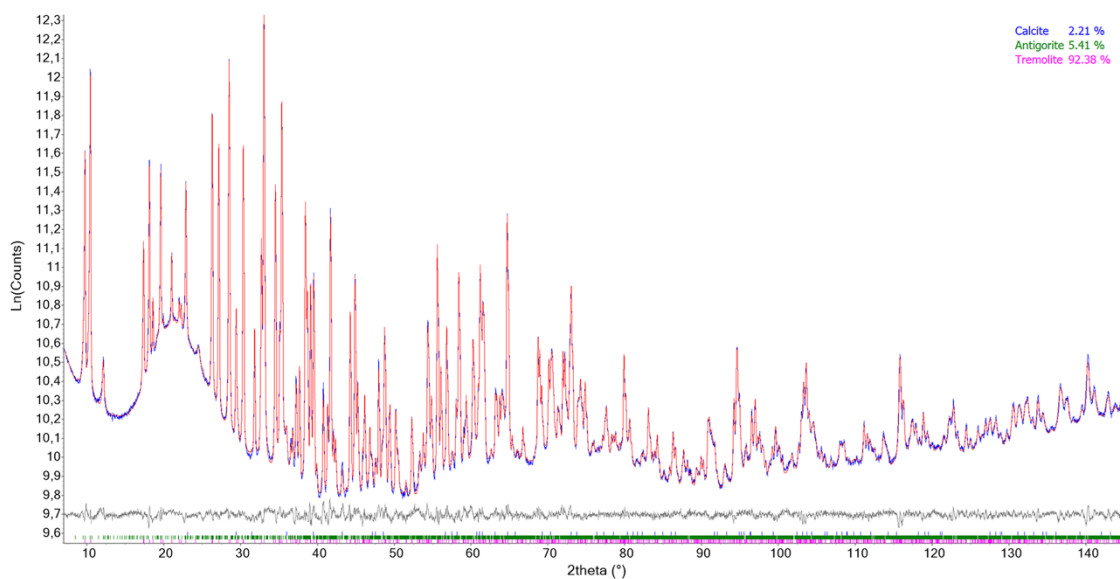


Figure 4. Rietveld plots of the refinement of tremolite. Intensity reported in logarithmic scale. Blue experimental; red: calculated; grey: difference plots; vertical bars indicate the position of the calculated Bragg reflections of (from above to below): calcite (blue), serpentine-like (green) and tremolite (magenta).

Table 2. ^{57}Fe Mössbauer parameters of the tremolite sample.

IS (mm/s)	QS (mm/s)	FWHM	Area (%)	Assignment	apfu Fe
1.140(3)	2.96(2)	0.25(2)	37(9)	$\text{Fe}^{2+} M(1)+M(3)$	0.109
1.158(7)	2.76(7)	0.33(3)	24(10)	$\text{Fe}^{2+} M(1)+M(3)$	
1.159(3)	1.90(1)	0.27(1)	26(5)	$\text{Fe}^{2+} M(2)+M(4)$	0.039
0.36(2)	0.60(3)	0.55(6)	14(3)	$\text{Fe}^{3+} M(2)$	0.024

Table 3. Cell parameters and volume of tremolite fibres and agreement factors (as defined in Young, 1993) of the Rietveld refinements.

	PL5
R_{Bragg} (%)	0.78
R_{wp} (%)	1.72
R_{p} (%)	1.30
GoF	2.93
DWd	0.41
a (Å)	9.84785(6)
b (Å)	18.06597(11)
c (Å)	5.28027(3)
β (Å)	104.7546(5)
Vol. (Å ³)	908.442(10)

Table 4. Quantitative Phase Analysis of the tremolite sample.

Phases	PL5
Tremolite	92.41(17)
Serpentine-like	5.41(16)
Calcite	2.19(5)

RESULTS AND DISCUSSION

Tremolite shows fibrous morphology and the single fibres, arranged to form bundles, appear straight and rigid with diameter well below 1 μm (Figure 2). Edges are often saw-teeth like, a feature that has been recently consistently observed in high magnification SEM images of fibres subjected to different types of weathering processes (Pacella et al., in preparation). SEM-EDS analyses revealed substantial chemical homogeneity of the fibres (Table 1). Besides, the variations observed for SiO_2 , MgO e CaO are very small (< ca. 4% relative), whereas for FeO_{tot} is of ca. 15% relative. The minor T deficiency is due to analytical error.

⁵⁷Fe Mössbauer spectroscopy of PL5 show a spectrum (Figure 3) with two well separated Fe^{2+} doublets and also a shoulder feature, typical for Fe^{3+} . The outer doublet shows slight asymmetry and was modelled with two doublets to improve fitting parameters. The inner Fe^{2+} doublet and the Fe^{3+} doublet could be accurately fitted with one doublet each. The assignment of doublets to structural site follow the model of Goldman (1979) and Andreozzi et al. (2009), with the outer doublet caused by Fe^{2+} in $M(1)+M(3)$, the

Table 5. Relevant bond distances (in Å) of tremolite fibres.

* Calculated as in Table 7 of Hawthorne and Oberti (2007).

		Pristine
$T(1)$	-O(7)	1.624(2)
	-O(6)	1.656(4)
	-O(1)	1.601(4)
	-O(5)	1.635(4)
< $T(1)$ -O>		1.629
$T(2)$	-O(4)	1.593(3)
	-O(5)	1.660(3)
	-O(2)	1.624(4)
	-O(6)	1.672(4)
< $T(2)$ -O>		1.637
$M(1)$	-O(3) x2	2.079(3)
	-O(1) x2	2.070(4)
	-O(2) x2	2.085(3)
< $M(1)$ -O>		2.078
$M(2)$	-O(4) x2	2.036(3)
	-O(2) x2	2.082(4)
	-O(1) x2	2.112(3)
< $M(2)$ -O>		2.077
$M(3)$	-O(1) x4	2.096(3)
	-O(3) x2	2.068(5)
< $M(3)$ -O>		2.087
<< $M(1,2,3)$ -O>>		2.081
<< $r^{M(1,2,3)}$ >>*		0.725
$M(4)$	-O(4) x2	2.315(4)
	-O(2) x2	2.397(3)
	-O(6) x2	2.549(3)
	-O(5) x2	2.751(3)
< $M(4)$ -O>		2.503

Table 6. Site scattering (s.s.) at A, B and C sites from Rietveld refinement.

Site	from refinement	from SEM-EDS
C		
<i>M</i> (1)	24.12(8)	24.56
<i>M</i> (2)	23.88(8)	24.52
<i>M</i> (3)	12.70(6)	12.97
$\Sigma_{M(1)+M(2)+M(3)}$	60.7(2)	62.04
B		
<i>M</i> (4)	39.27(10)	39.74
<i>A</i> (2/ <i>m</i>)	1.02(6)	1.36

inner doublet to Fe^{2+} in *M*(2)+*M*(4), and the shoulder doublet to Fe^{3+} in *M*(2) site (Figure 3, Table 2). Despite that the outer doublet was fitted with two doublets set, a distribution of Fe^{2+} over the *M*(1) and *M*(3) sites cannot be ascertained due to lack of spectral resolution, stemming for the structural similarity of these two sites.

The following crystal-chemical formula was derived by combining chemical and Mössbauer data: ${}^A\text{Na}_{0.124}{}^B(\text{Ca}_{1.922}\text{Na}_{0.003}\text{Fe}^{2+}_{0.026}\text{Mg}_{0.049})_{\Sigma=2.000}{}^C(\text{Fe}^{2+}_{0.122}\text{Fe}^{3+}_{0.024}\text{Mg}_{4.854})_{\Sigma=5.000}{}^T(\text{Si}_{7.946}\text{Al}_{0.024})_{\Sigma=7.970}\text{O}_{22}\text{O}^{(3)}(\text{OH})_{2.000}$. Fe^{2+} partition between *M*(2) and *M*(4) was performed from structural analysis results and crystal chemical reasonings (see below).

The sample shows Ca/ Σ M ratio and composition very close to that of the end-member tremolite, ideally ${}^A\text{Ca}_2{}^B\text{Ca}_2{}^C\text{Mg}_5{}^T\text{Si}_8\text{O}_{22}\text{O}^{(3)}(\text{OH})_2$. In addition, the % ferro-actinolite content [$(\text{Fe}^{2+}+\text{Mn})/(\text{Fe}^{2+}+\text{Mn}+\text{Mg})$] is of ca. 3%. The values of cell parameters and volume (Table 3) confirm the occurrence of limited Fe^{2+} content (Vignaroli

et al., 2014).

QPA indicates that serpentine-like phase(s) and calcite account for ca. 7.5 wt% of the mixture (Table 4). However, due to the simplification adopted for modelling the structure of serpentine-like phase(s), large uncertainties are expected to affect its/their quantification. In particular, significant overestimation is plausible owing to the observed marked broadening of the reflections of antigorite caused by the attempt to compensate for structural model deficiencies. Accordingly, the possible contribution to the Mössbauer spectrum of the accessory phases is negligible.

As far as tremolite structure is referred to, $\langle T(2)\text{-O} \rangle$ of 1.637 Å is slightly longer than 1.629 Å of $\langle T(1)\text{-O} \rangle$ in agreement with the very small Al content allocated at *T*(1) (Table 5). $\langle M(3)\text{-O} \rangle$ is significantly longer (2.087 Å) than $\langle M(1)\text{-O} \rangle$ and $\langle M(2)\text{-O} \rangle$ (2.078 and 2.077 Å, respectively) suggesting a preferential allocation of Fe^{2+} at *M*(3) (Table 5). Cation partition at C-site was performed following the procedure of Vignaroli et al. (2014) (Tables 6, 7) involving an iterative optimization of both site scattering (s.s.) and aggregate sizes of the constituent cations $\langle r^M \rangle$ at the various *M*(1,2,3) sites. Following this approach, Fe^{2+} assigned to *M*(2)+*M*(4) from Mössbauer spectroscopy has been prevalently allocated at *M*(4) in a 1:2 proportion, in agreement with the strong temperature-dependent preference of iron for this site in Ca-amphiboles (Skogby and Annersten, 1985) and with the well-known $M(3) > M(1) \gg M(2)$ C-site preference of ferrous iron (Oberti et al., 2007). As a result, the s.s. at C-site derived from the refinement returns a total of 60.7(2) e^- which is moderately smaller than 62.04 e^- obtained from SEM-EDS (Table 6). More in detail, s.s. at *M*(2) [23.88(8) e^-] is apparently consistent with the occurrence of vacancies (24 e^- =2 apfu Mg). The general underestimation of s.s. at C-site has been previously reported in literature as an artifact (Vignaroli et al., 2014), possibly arising from correlation between sof of

Table 7. Cation partition at A, B and C sites from Rietveld refinement.

Site	Cation partition	$\langle r^M \rangle$ from bond distances	$\langle r^M \rangle$ from partition
C			
<i>M</i> (1)	$\text{Mg}_{1.960}\text{Fe}^{3+}_{0.000}\text{Fe}^{2+}_{0.040}$	0.718	0.721
<i>M</i> (2)	$\text{Mg}_{1.963}\text{Fe}^{3+}_{0.024}\text{Fe}^{2+}_{0.013}$	0.717	0.719
<i>M</i> (3)	$\text{Mg}_{0.931}\text{Fe}^{3+}_{0.000}\text{Fe}^{2+}_{0.069}$	0.727	0.724
$\Sigma_{M(1)+M(2)+M(3)}$	$\text{Mg}_{4.854}\text{Fe}^{3+}_{0.024}\text{Fe}^{2+}_{0.122}$		
B			
<i>M</i> (4)	$\text{Ca}_{1.922}\text{Na}_{0.003}\text{Mg}_{0.049}\text{Fe}^{2+}_{0.026}$		
<i>A</i> (2/ <i>m</i>)	$\text{Na}_{0.124}$		

M- (and *A*-) sites and absorption correction (Ballirano et al., 2017). Moreover, the underestimation has been shown to be prevalently taken up by the *M*(2) site (Ballirano and Pacella, 2020). Present data support this observation as the largest discrepancy is observed at *M*(2) and secondarily at *M*(1). Refined s.s. at *M*(4) is underestimated as compared to that from site partition. It is worth noting that the presence of ^B(Mg, Fe²⁺, Mn²⁺)-constituents, that in the studied sample corresponds to ^B(Mg+Fe²⁺)=0.075 apfu, might be related to the presence of a split *M*(4') site. However, any attempt to refine a site at ca. (0, 0.246, 1/2), corresponding to the expected position of *M*(4'), failed, possibly because of the inability of the data to support the optimization of such subtle static disorder.

Refined s.s. at *A*-site is in reasonable agreement with that obtained from SEM-EDS despite the simplification of modelling it as a single *A*(2/*m*) one.

Table 7 summarizes the cation partition based on combined SEM-EDS, XRPD and Mössbauer data. The discrepancies among the various $\langle r^M \rangle$, calculated from bond distances and cation partition, are small being within ± 0.003 Å. The following empirical formula was obtained: $A(Na_{0.124})_{\Sigma 0.124} M^{(4)}(Ca_{1.922}Na_{0.003}Fe^{2+}_{0.026}Mg_{0.049})_{\Sigma 2.000} [M^{(1)}(Mg_{1.960}Fe^{2+}_{0.040})_{\Sigma 2.000} M^{(2)}(Mg_{1.963}Fe^{3+}_{0.024}Fe^{2+}_{0.013})_{\Sigma 2.000} M^{(3)}(Mg_{0.931}Fe^{2+}_{0.069})_{\Sigma 1.000}] [T^{(1)}(Si_{3.946}Al_{0.024})_{\Sigma 3.970} T^{(2)}(Si_{4.000})O_{22} O^{(3)}(OH_{2.000})_{\Sigma 2.000}$.

CONCLUSIONS

This work reports a detailed crystal-chemical and structural characterization of a sample of asbestos tremolite from an abandoned serpentine quarry located in Mount Reventino (Calabria, Italy). The chemical formula and the cation distribution, obtained by integrating SEM-EDS, XRPD and Mössbauer data, show that the investigated sample is very close to tremolite end member, owing to its very low Fe content (ferro-actinolite component of ca. 3%). It must be noted that both presence of Fe and its coordination environment within the structure play a key role in fibre toxicity (Hardy and Aust, 1995; Kamp, 2009; Liu et al., 2013). Moreover, it has been demonstrated that chemical reactivity of asbestos depends on specific Fe sites lying at the surface rather than the total Fe content of the mineral phases (Turci et al., 2011; Andreozzi et al., 2017; Pacella et al., 2018). On this basis, the presence of Fe bearing asbestos tremolite in the investigated area may represent a potential hazard for human health.

It should be noted that tremolite fibres of this work represent a good candidate sample for investigating and modelling their chemical reactivity because of the excellent purity, chemical homogeneity and the availability of detailed crystal chemical and structural data. As a further interesting peculiarity, the sample has some Fe²⁺ allocated at *M*(4), condition that might alter its rate of dissolution

and modulate iron availability for surface reactions as compared to other tremolite fibres samples that do not share this feature. Such experiments are currently in progress. Besides, in order to accurately assess the NOA risk, studies aimed at investigating the extent of the NOA-bearing outcrops and the amount of fibres that could be released, following disturbance of rocks and soils, need to be improved. In this regard, a mapping of the NOA in Calabrian ophiolites was carried out in order to identify safety procedures and control measures to reduce a possible exposure arising from human activities in those areas where fibrous minerals were detected (Campopiano et al., 2018). Environmental air pollution of tremolite fibres in the Mount Reventino area was confirmed by a study on lung tissue of animals living thereby (Campopiano et al., 2020). Indeed, the abundant presence of fibers of tremolite in the lungs of the investigated animals confirmed the successful spread of mineral fibers in the environment coming from NOA.

ACKNOWLEDGEMENTS

The research received financial support by INAIL, BRIC ID 57/2019.

REFERENCES

- Addison J. and McConnel E.E., 2005. A review of carcinogenicity studies of asbestos and non asbestos tremolite and other amphiboles. International Symposium on the Health Hazard Evaluation of Fibrous Particles associated with Taconite and the adjacent Duluth Complex.
- Alvarez W., 2005. Structure of the Monte Reventino greenschist folds: a contribution to untangling the tectonic-transport history of Calabria, a key element in Italian tectonics. *Journal of Structural Geology* 27, 1355-1378.
- Amodio Morelli L., Bonardi G., Colonna V., Dietrich D., Giunta G., Ippolito F., Liguori V., Lorenzoni S., Paglionico A., Perrone V., et al., 1976. L'arco calabro peloritano nell'orogene appenninico Magrebide [Calabrian peloritane arc in the apennine orogene maghrebide]. *Memorie della Società Geologica Italiana* 17, 1-60.
- Andreozzi G.B., Ballirano P., Gianfagna A., Mazziotti-Tagliani S., Pacella A., 2009. Structural and spectroscopic characterization of a suite of fibrous amphiboles with high environmental and health relevance from Biancavilla (Sicily, Italy). *American Mineralogist* 94, 1333-1340.
- Andreozzi G.B., Pacella A., Corazzari I., Tomatis M., Turci F., 2017. Surface reactivity of amphibole asbestos: a comparison between crocidolite and tremolite. *Scientific Reports* 7, 14696.
- Ballirano P., 2003. Effects of the choice of different ionization level for scattering curves and correction for small preferred orientation in Rietveld refinement: the MgAl₂O₄ test case. *Journal of Applied Crystallography* 36, 1056-1061.
- Ballirano P., Andreozzi G.B., Belardi G., 2008. Crystal chemical

- and structural characterization of fibrous tremolite from Susa Valley, Italy, with comments on potential harmful effects on human health. *American Mineralogist* 93, 1349-1355.
- Ballirano P., Bloise A., Gualtieri A.F., Lezzerini M., Pacella A., Perchiazzi N., Dogan M., Dogan A.U., 2017. The crystal structure of mineral fibres. In: A.F. Gualtieri (Ed.) "Mineral fibres: crystal chemistry, chemical-physical properties, biological interaction and toxicity". European Mineralogical Union, London, pp. 17-64.
- Ballirano P. and Pacella A., 2020. Towards a detailed comprehension of the inertisation processes of amphibole asbestos: in situ high-temperature behaviour of fibrous tremolite. *Mineralogical Magazine* 84, 888-899.
- Bloise A., Critelli T., Catalano M., Apollaro C., Miriello D., Croce A., Barrese E., Liberi F., Piluso E., Rinaudo C., Belluso E., 2014. Asbestos and other fibrous minerals contained in the serpentinites of the Gimigliano-Mount Reventino unit (Calabria, S-Italy). *Environmental Earth Sciences* 71, 3773-3786.
- Bloise A., Punturo R., Catalano M., Miriello D., Cirrincione R., 2016. Naturally occurring asbestos (NOA) in rock and soil and relation with human activities: the monitoring example of selected sites in Calabria (southern Italy). *Italian Journal of Geosciences* 135, 268-279.
- Bruker AXS, 2016. Topas V6: General profile and structure analysis software for powder diffraction data. Bruker AXS, Karlsruhe, Germany.
- Burrigato F., Ballirano P., Fiori S., Papacchini L., Sonno M., 2001. Segnalazione di tremolite asbestiforme nel Lazio. *Il Cercapietre Notiziario del Gruppo Mineralogico Romano* 1-2, 33-35.
- Burrigato F., Gaglianone G., Gerbasi G., Mazziotti-Tagliani S., Papacchini L., Rossini F., Sperduto B., 2010. Fibrous mineral detection in natural soil and risk mitigation (1st paper). *Periodico di Mineralogia* 79, 3, 21-35.
- Campopiano A., Olori A., Spadafora A., Rosaria Bruno M., Angelosanto F., Iannò A., Casciardi S., Giardino R., Conte M., Oranges T., Iavicoli S., 2018. Asbestiform minerals in ophiolitic rocks of Calabria (southern Italy). *International Journal of Environmental Health Research* 28, 134-146
- Campopiano A., Cannizzaro A., Olori A., Angelosanto F., Bruno M.R., Sinopoli F., Bruni B.M., Casalnuovo F., Iavicoli S., 2020. Environmental contamination by naturally occurring asbestos (NOA): Analysis of sentinel animal lung tissue. *Science of the Total Environment* 745, 140990.
- Capitani G. and Mellini M., 2004. The modulated crystal structure of antigorite: The m=17 polysome. *American Mineralogist* 89, 147-158.
- Cavallo A. and Rimoldi B., 2013. Chrysotile asbestos in serpentinite quarries: A case study in Valmalenco, central alps, northern Italy. *Environmental Sciences: Processes and Impacts* 15, 1341-1350.
- Cirrincione R., Fazio E., Fiannacca P., Ortolano G., Pezzino A., Punturo R., 2015. The Calabria-Peloritani Orogen, a composite terrane in Central Mediterranean; its overall architecture and geodynamic significance for a pre-Alpine scenario around the Tethyan basin. *Periodico di Mineralogia*, 84(3B), Special Issue, 701-749.
- Davis J.M.G., Addison J., McIntosh C., Miller B.G., Niven K., 1991. Variations in the carcinogenicity of tremolite dust samples of differing morphology. *Annals of the New York Academy of Sciences* 643, 473-490.
- Decree of the Environment Ministry, 18 March 2003 n°101, 2003. Regolamento per la realizzazione di una mappatura delle zone del territorio nazionale interessate dalla presenza di amianto, ai sensi dell'articolo 20 della legge 23 marzo 2001, n 93 [Regulation for mapping areas of the national territory affected by the asbestos presence, in accordance with Law no 93, art20]. *Official Gazette of the Italian Republic, General Series* n.106, 9 May 2003.
- Gualtieri F., 2020. Naturally Occurring Asbestos: A Global Health Concern? State of the Art and Open Issues. *Environmental and Engineering Geoscience* 26, 3-8.
- Hardy J.A. and Aust A.E., 1995. Iron in asbestos chemistry and carcinogenicity. *Chemical Reviews* 95, 97-118.
- Harper M., 2008. 10th anniversary critical review: Naturally occurring asbestos. *Journal of Environmental Monitoring*, Vol. 10, No. 12, 1394-1408.
- Hawthorne F.C., Oberti R., Harlow G.E., Maresch W.V., Martin R.F., Schumacher J.C., Welch M.D., 2012. Nomenclature of the amphibole supergroup. *American Mineralogist* 97, 2031-2048.
- Järvinen M., 1993. Application of symmetrized harmonics expansion to correction of the preferred orientation effect. *Journal of Applied Crystallography* 26, 525-531.
- Kamp D.W., 2009. Asbestos-induced lung diseases: an update. *Translational Research*, 153, 143-152.
- Langer A.M., 2008. Identification and enumeration of asbestos fibers in the mining environment: Mission and modification to the Federal Asbestos Standard. *Regulatory Toxicology and Pharmacology* 52, S207-S217.
- Lee R.J., Strohmeier B.R., Bunker K.L., Van Orden D.R., 2008. Naturally occurring asbestos - A recurring public policy challenge: *Journal of Hazardous Materials* 153, 1-21.
- Liu G., Cheresch, P., Kamp D.W., 2013. Molecular Basis of Asbestos-Induced Lung Disease. *Annual Review of Pathology: Mechanisms of Disease* 8, 161-187.
- Marinos P., Hoek E., Marinos V., 2006. Variability of the engineering properties of rock masses quantified by the geological strength index: the case of ophiolites with special emphasis on tunnelling. *Bulletin of Engineering Geology and the Environment* 65, 129-142.
- Maslen E.N., Streltsov V.A., Streltsova N.R., 1993. X-ray study of the electron density in calcite, CaCO₃. *Acta Crystallographica* B49, 636-641.
- Nichols M.D., Young, D., Davis, G., 2002. Guidelines for

- geologic investigation of naturally occurring asbestos in California. In Clinkenbeard J.P., Churchill R.K., Lee K. (Eds.), California geological survey public information offices. Special publication 124. <http://www.consrv.ca.gov>.
- Oberti R., Cámara F., Della Ventura G., Iezzi G., Benimoff A.I., 2006. Parvo-mangano-edenite and parvo-mangano- tremolite two new Group 5 monoclinic amphiboles from Fowler, New York, and comments on the solid solution between Ca and Mn²⁺ at the M4 site. *American Mineralogist*, 91, 526-532.
- Oberti R., Cannillo E., Hawthorne F.C., Ungaretti L., 1993. The behaviour of Mn in amphiboles: Mn in richterite. *European Journal of Mineralogy* 5, 43-51.
- Oberti R. and Ghose S., 1993. Crystal-chemistry of a complex Mn-bearing alkali amphibole ("tirodite") on the verge of exsolution. *European Journal of Mineralogy* 5, 1153-1160.
- Oberti R., Hawthorne F.C., Cannillo E., Cámara F., 2007. Long-range order in amphiboles. In Hawthorne F.C., Oberti R., Della Ventura G., Mottana A. (Eds.), *Amphiboles: Crystal chemistry, occurrence, and health issues. Reviews in Mineralogy and Geochemistry*, Mineralogical Society of America, Chantilly, Virginia, USA, 67, 125-171.
- Ogniben L., 1969. Schema introduttivo alla geologia del confine Calabro-Lucano [Introductory pattern to geology of the Calabro-Lucano border]. *Memorie della Società Geologica Italiana* 8, 458-768.
- Pacella A., Andreozzi G.B., Fournier J., 2010. Detailed crystal chemical study and iron topochemistry of asbestos in its natural setting: a first step to understanding its chemical reactivity. *Chemical Geology* 277, 197-206.
- Pacella A., Andreozzi G.B., Corazzari I., Tomatis M., Turci F., 2018. Surface reactivity of amphibole asbestos: a comparison between two tremolite samples with different surface area. *Periodico di Mineralogia* 87, 195-205.
- Pacella A., Tomatis M., Viti C., Bloise A., Arrizza L., Ballirano P., Turci F., 2020. Thermal inertization of amphibole asbestos modulates Fe topochemistry and surface reactivity. *Journal of Hazardous Materials* 398, 123119.
- Pan X.L., Day H.W., Wang W., Beckett L.A., Schenker M.B., 2005. Residential proximity to naturally occurring asbestos and mesothelioma risk in California: *American Journal of Respiratory and Critical Care Medicine* 172, 1019-1025.
- Pasetto R., Bruni B.M., Bruno C., Cauzillo G., Cavone D., Convertini L., De Mei B., Marconi A., Montagnano G., Musti M., Paoletti L., Comba P., 2004. Mesotelioma pleurico ed esposizione ambientale a fibre minerali: il caso di un'area rurale in Basilicata. *Annali dell'Istituto Superiore di Sanità* 40, 251-265.
- Pereira D., Yenes M., Blanco J.A., Peinado M., 2007. Characterization of serpentinites to define their appropriate use as dimension stone. In: Příkryl R. and Smith B.J. (Eds.), *Building stone decay: from diagnosis to conservation*. Geological Society London Special Publications 271, 55-62.
- Piluso E., Cirrincione R., Morten L., 2000. Ophiolites of the Calabrian Peloritan arc and their relationships with the crystalline basement (Catena Costiera and Sila Piccola, Calabria, Southern Italy). *GLOM 2000 Excursion GuideBook. Ofioliti* 25, 117-140.
- Prescher C., McCammon C., Dubrowinsky L. 2012. MossA: a program for analyzing energy-domain Mössbauer spectra from conventional and synchrotron sources. *Journal of Applied Crystallography* 45, 329-331.
- Punturo R., Bloise A., Critelli T., Catalano M., Fazio E., Apollaro C., 2015. Environmental implications related to natural asbestos occurrences in the ophiolites of the Gimigliano-Mount Reventino Unit (Calabria, Southern Italy). *International Journal of Environmental Research* 9, 405-418.
- Ross M. and Nolan R.P., 2003. History of asbestos discovery and use and asbestos-related disease in context with the occurrence of asbestos within ophiolite complexes. *Special Papers - Geological Society of America* 373, 447-470.
- Sabine T.M., Hunter B.A., Sabine W.R., Ball C.J., 1998. Analytical expressions for the transmission factor and peak shift in absorbing cylindrical specimens. *Journal of Applied Crystallography* 31, 47-51.
- Skogby H. and Annersten H., 1985. Temperature dependent Mg-Fe-cation distribution in actinolite-tremolite. *Neues Jahrbuch für Mineralogie Monatshefte* 1985, 193-203.
- Stephens P.W., 1999. Phenomenological model of anisotropic peak broadening in powder diffraction. *Journal of Applied Crystallography* 32, 281-289.
- Turci F., Tomatis M., Lesci I.G., Roveri N., Fubini B., 2011. The iron-related molecular toxicity mechanism of synthetic asbestos nanofibres: a model study for high-aspect-ratio nanoparticles. *Chemistry* 17, 350-358.
- Vignaroli G., Ballirano P., Belardi G., Rossetti F., 2014. Asbestos fibre identification vs. evaluation of asbestos hazard in ophiolitic rock mélanges, a case study from the Ligurian Alps (Italy). *Environmental and Earth Sciences* 72, 3679-3698.
- Vignaroli G., Rossetti F., Belardi G., Billi A., 2011. Linking rock fabric to fibrous mineralisation: A basic tool for the asbestos hazard. *Natural Hazards and Earth System Sciences* 11, 1267-1280.
- Vitale S., Fedele L., Tramparulo F., Ciarcia S., Mazzoli S., Novellino A., 2013. Structural and petrological analyses of the Frido Unit (southern Italy): new insights into the early tectonic evolution of the southern Apennines-Calabrian Arc system. *Lithos* 168-169, 219-235.
- Young R.A., 1993. Introduction to the Rietveld method: In: R.A. Young (Ed.) "The Rietveld method". Oxford University Press, pp. 1-38.



This work is licensed under a Creative Commons Attribution 4.0 International License CC BY. To view a copy of this license, visit <http://creativecommons.org/licenses/by/4.0/>